

# Quasi-elastic scattering under short-range order: the linear regime and beyond

Michael Leitner and Gero Vogl

Universität Wien, Fakultät für Physik, Strudlhofgasse 4, 1090 Wien, Austria

E-mail: [michael.leitner@univie.ac.at](mailto:michael.leitner@univie.ac.at)

Received 14 January 2011, in final form 22 March 2011

Published 8 June 2011

Online at [stacks.iop.org/JPhysCM/23/254206](http://stacks.iop.org/JPhysCM/23/254206)

## Abstract

Incoherent quasi-elastic scattering of neutrons or gamma rays determines the jump vectors of diffusing single atoms. Coherent quasi-elastic scattering beyond that contains additional information on the interaction between atoms. Here we firstly derive the influence of weak interactions (i.e. the high-temperature limit) on the correlation times taking an analytical approach via transition state theory, different from and, in our opinion, easier to follow than the lattice dynamics approach by Sinha and Ross. As de Gennes had already argued earlier, short-range order increases the correlation time (or equivalently narrows the quasi-elastic line) proportional to the diffuse intensity at the corresponding wavevector transfer. Secondly we show by way of Monte Carlo simulations that for strong interactions the deviations from the analytical theory bear additional information about the jump processes. We compare our theory with the results of a recent XPCS experiment.

(Some figures in this article are in colour only in the electronic version)

## 1. Introduction

The mechanisms of diffusion on the atomic scale can be studied by the scattering of quanta with appropriate wavelengths (Petry and Vogl, 1987). This includes the classical methods of quasi-elastic neutron scattering (QENS, Springer and Lechner, 2005) and Mößbauer spectroscopy (MS, Vogl and Sepiol, 2005), and the modern synchrotron-based methods of nuclear resonant scattering (NRS, Vogl and Sepiol, 2005) and, most recently, x-ray photon correlation spectroscopy (XPCS). We will subsume these methods under the term quasi-elastic methods, as they either directly measure small energy transfers between the sample and the scattered quanta (QENS and MS), or the Fourier-dual case of the decay of correlations in the time domain of the scattered radiation. These methods give the jump vectors and jump frequencies of the atoms, allowing a picture to be drawn up of the mechanisms on the atomic scale leading to the macroscopic spreading of concentrations.

The quasi-elastic methods can be further classified into belonging to the coherent or incoherent groups. This distinction can most easily be clarified by asking whether a given method detects a direct exchange between two atoms of the same element (i.e. whether such an event leads to a broadening in energy or a loss of correlation in time): For the cases of MS

and NRS each resonant atom is excited with a phase defined by its position along the direction of the incoming radiation. When two atoms exchange their positions, they keep their phases, leading to a disruption of the coherence of the excited atoms in the sample and therefore to a loss of correlation and a broadening in energy. MS and NRS are therefore incoherent methods. The scattering of non-resonant x-rays, on the other hand, only depends on the electronic density in the sample and therefore on the chemical configuration. These are not affected by exchanging two atoms of the same element, so XPCS is a coherent method. With QENS the distinction is not so clear, however. Atoms of a given element can have different neutron scattering lengths by being of a different isotope or differing in the nuclear spin. This leads in general to a superposition of scattering of coherent and incoherent characteristics. Fine-tuning the isotopical composition of the sample or investigating elements where the natural isotopical composition is favourable often allows one contribution to dominate. The greater part of experimental investigations have focussed on incoherent scattering, probably because the results from an incoherent experiment have a more intuitive interpretation. This is unfortunate in our opinion, because incoherent scattering gives information about quantities of atoms without regard to their surroundings, whereas the effect of interference

between the scattering emanating from neighbouring atoms as encountered in coherent scattering allows the atoms' dynamical behaviour to be differentiated by their surroundings in a certain way, as we will show. With the upcoming method of XPCS being an inherently coherent method the need for more clearly elucidating the connection between the atomic-scale events and the coherently scattered signal is obvious. This is our aim in this publication.

It is structured as follows: After this introduction we will first define the theoretical concepts relevant to coherent quasi-elastic scattering techniques. Then we will give a derivation of the coherent correlation times/quasi-elastic linewidths resulting from the diffusion of interacting particles on a Bravais lattice in the limit of weak interactions, i.e. weak short-range order. We will use only basic probability theory and fundamental physical concepts such as site occupations and transition frequencies with the intention to enable even non-experts to follow the arguments. We will then investigate the regime of stronger interactions by way of computer experiments and demonstrate that the deviations from the linear theory contain valuable information about the atomic jump mechanisms that are otherwise inaccessible. Finally we will interpret the findings from a recent XPCS-experiment in view of these results and speculate about future possibilities.

## 2. Outline of the problem

In the following we will treat certain aspects of diffusion on a Bravais lattice. For the most part we will use the setting of a number of identical diffusing particles on a partly filled lattice, a physical example would be interstitial hydrogen diffusion (Cook et al., 1990). We want to note that the case of a binary alloy, where the lattice sites are occupied by either an A or a B atom and the occupancy of neighbouring sites is randomly exchanged, is equivalent: substituting holes for the B atoms only changes the scattering by a constant factor (outside of the Bragg reflections).

The aspect of the sample dynamics that is probed by coherent quasi-elastic methods is most intuitively put in terms of the time-dependent pair-correlation function  $G(\Delta\vec{x}, \Delta t)$ . This concept goes back to van Hove (1954), in the classical case it gives the probability to find a particle at position  $\vec{x} + \Delta\vec{x}$  and time  $t + \Delta t$  under the condition that there was a particle at position  $\vec{x}$  and time  $t$ . Fourier-transforming  $G(\Delta\vec{x}, \Delta t)$  in space gives the so-called intermediate scattering function  $I(\vec{q}, \Delta t)$ , which is directly accessed by scattering methods working in the time domain such as XPCS. An additional transform over time gives the scattering function  $S(\vec{q}, \omega)$ , appropriate for scattering methods in the energy domain (e.g., QENS). Our task here is then to connect the atomic-scale dynamics with the resulting  $G(\Delta\vec{x}, \Delta t)$  or equivalently  $I(\vec{q}, \Delta t)$  or  $S(\vec{q}, \omega)$ .

We describe the state of the system by  $\sigma$ , the occupation function of the lattice sites:  $\sigma(\vec{x}) = 1$  if lattice site  $\vec{x}$  is occupied by a particle, otherwise  $\sigma(\vec{x}) = 0$ . The expected value of the occupation at any point is given by the concentration of particles  $c$ . We define  $A$  as the Fourier transform of  $\sigma$  (the naming should suggest to view  $A(\vec{q})$  as scattering amplitude).

We therefore have

$$G(\Delta\vec{x}, \Delta t) = \langle \sigma(\cdot, \cdot) \sigma(\cdot + \Delta\vec{x}, \cdot + \Delta t) \rangle \quad (1)$$

and

$$I(\vec{q}, \Delta t) = \langle A(\vec{q}, \cdot) \bar{A}(\vec{q}, \cdot + \Delta t) \rangle. \quad (2)$$

Assuming pair potentials, the Hamiltonian is given by

$$H(\sigma) = \sum_{\vec{x} \neq \vec{y}} V(\vec{x} - \vec{y}) \sigma(\vec{x}) \sigma(\vec{y}). \quad (3)$$

This is equivalent to the case of a binary system, with  $V$  the so-called effective pair potential.

In the following section we will show that for weak interactions, given an initial amplitude, diffusion leads to an exponential regression of the expected value of the amplitude towards zero:

$$\frac{d}{dt} \langle A(\vec{q}, t) \rangle = -A(\vec{q}, t) \Gamma_{\text{coh}}(\vec{q}) \quad (4)$$

This gives

$$\langle A(\vec{q}, t + \Delta t) \rangle = A(\vec{q}, t) e^{-\Gamma_{\text{coh}}(\vec{q}) \Delta t} \quad (5)$$

and

$$I(\vec{q}, \Delta t) = \langle A(\vec{q}, \cdot) \bar{A}(\vec{q}, \cdot) \rangle e^{-\Gamma_{\text{coh}}(\vec{q}) \Delta t} = I_{\text{SRO}}(\vec{q}) e^{-\Gamma_{\text{coh}}(\vec{q}) \Delta t}. \quad (6)$$

$\Gamma_{\text{coh}}(\vec{q})$  is therefore the experimentally accessed quantity in a coherent quasi-elastic experiment, i.e. the inverse of the correlation time for time-domain methods or the linewidth (after multiplication by the Planck constant) for energy-domain methods.  $I_{\text{SRO}}$  is the expected value of the scattered intensity due to short-range order.

## 3. The linear theory

Here we obtain a simple expression for the coherent linewidth  $\Gamma_{\text{coh}}(\vec{q})$  under the assumption of weak interactions. Note that this is a rederivation of a result already given by Sinha and Ross (1988), who used a general framework of lattice dynamics. Our derivation avoids the need of treating phonons explicitly by using transition state theory.

We define

$$\Delta U(\vec{x}_1, \vec{x}_2, \sigma) = 2 \sum_{\Delta\vec{x}} V(\Delta\vec{x}) (\sigma(\vec{x}_2 + \Delta\vec{x}) - \sigma(\vec{x}_1 + \Delta\vec{x})), \quad (7)$$

that is the difference in energy between a state with  $\sigma(\vec{x}_1) = 1$  and  $\sigma(\vec{x}_2) = 0$  and a state with  $\sigma(\vec{x}_1) = 0$  and  $\sigma(\vec{x}_2) = 1$ . In other words, it is the energy gained when moving a particle from  $\vec{x}_1$  to  $\vec{x}_2$ , with the occupations of all the other sites given by  $\sigma$ .

Classical transition state theory (Vineyard, 1957) gives for the transition frequency from a stable state  $\sigma_1$  (a local minimum in the energy surface) to a stable state  $\sigma_2$

$$v'(\sigma_1 \rightarrow \sigma_2) = \frac{\omega(\sigma_1)}{\omega_S(\sigma_1 \leftrightarrow \sigma_2)} \exp\left(-\frac{H_S(\sigma_1 \leftrightarrow \sigma_2) - H(\sigma_1)}{k_B T}\right), \quad (8)$$

where  $H(\sigma_1)$  is the energy of the state  $\sigma_1$  with  $\omega(\sigma_1)$  the product of the frequencies of the normal modes, and  $H_S(\sigma_1 \leftrightarrow \sigma_2)$  is the energy at the saddle point of the transition path with  $\omega_S(\sigma_1 \leftrightarrow \sigma_2)$  the product of the modes resulting in displacements perpendicular to the transition path. We assume that the influence of the neighbouring occupations on the modes (that is on the jump entropy) can be neglected.

In our special case of a particle jumping on a lattice from  $\vec{x}_1$  to  $\vec{x}_2$  it is convenient to rearrange the general expression (8) into a constant factor  $v_{\vec{x}_2-\vec{x}_1}$  that includes the product of the normal mode frequencies and the Boltzmann factor of the mean saddle point energy of this jump type, and into a factor that includes the deviations due to the actual configuration  $\sigma$ . To be specific, we count the saddle point energy relative to the average of the energies of the initial and final state and denote the deviations from this value by  $\Delta E_S(\vec{x}_1, \vec{x}_2, \sigma)$ . We therefore arrive at the expression for the transition frequency

$$v'(\vec{x}_1 \rightarrow \vec{x}_2, \sigma) = v_{\vec{x}_2-\vec{x}_1} e^{-\frac{\Delta U(\vec{x}_1, \vec{x}_2, \sigma)}{2k_B T}} e^{-\frac{\Delta E_S(\vec{x}_1, \vec{x}_2, \sigma)}{k_B T}}, \quad (9)$$

where  $v_{\vec{x}_2-\vec{x}_1}$  depends only on the jump vector (and on temperature via the Boltzmann factor), but not on the actual configurations.

The flux of particles between  $\vec{x}_1$  and  $\vec{x}_2$  for arbitrary  $\sigma$  is therefore given by

$$\begin{aligned} F_{\vec{x}_1 \rightarrow \vec{x}_2} &= v_{\vec{x}_2-\vec{x}_1} e^{-\frac{\Delta E_S(\vec{x}_1, \vec{x}_2, \sigma)}{k_B T}} \left( \sigma(\vec{x}_2)(1 - \sigma(\vec{x}_1)) e^{\frac{\Delta U(\vec{x}_1, \vec{x}_2, \sigma)}{2k_B T}} \right. \\ &\quad \left. - \sigma(\vec{x}_1)(1 - \sigma(\vec{x}_2)) e^{-\frac{\Delta U(\vec{x}_1, \vec{x}_2, \sigma)}{2k_B T}} \right) \\ &= v_{\vec{x}_2-\vec{x}_1} \left( (\sigma(\vec{x}_2) - \sigma(\vec{x}_1)) \left( 1 - \frac{\Delta E_S(\vec{x}_1, \vec{x}_2, \sigma)}{k_B T} \right) \right. \\ &\quad \left. + \frac{\Delta U(\vec{x}_1, \vec{x}_2, \sigma)}{2k_B T} (\sigma(\vec{x}_1) + \sigma(\vec{x}_2) - 2\sigma(\vec{x}_1)\sigma(\vec{x}_2)) \right. \\ &\quad \left. + O((E/k_B T)^2) \right). \end{aligned} \quad (10)$$

Here  $E$  is a measure for the typical energy variations in both the saddle point and the stable positions, i.e.  $\Delta U(\vec{x}_1, \vec{x}_2, \sigma) = O(E)$  and  $\Delta E_S(\vec{x}_1, \vec{x}_2, \sigma) = O(E)$ .

Now we will do a mean-field approximation, so we take a random sample of  $N$  states (i.e. systems) from the canonical ensemble. We assume  $N$  to be large, so we need only consider terms of the leading order of deviations from the ensemble average (i.e. of the order  $O(N^{-1/2})$ ). We will also drop all quantities of order  $O((E/k_B T)^2)$ . We note that assuming the system to be only short-range ordered means

$$\langle \sigma(\vec{x})\sigma(\vec{y}) \rangle - \langle \sigma(\vec{x}) \rangle \langle \sigma(\vec{y}) \rangle = O(E/k_B T) \quad (11)$$

for  $\vec{x} \neq \vec{y}$ . Such products come up as the expressions for the energies are linear functionals in  $\sigma$ . We further note that due to ignoring terms of order  $O(1/N)$  we have

$$\begin{aligned} \langle \sigma(\vec{x}) \rangle \langle \sigma(\vec{x}) \rangle &= \left( c + (\langle \sigma(\vec{x}) \rangle - c) \right) \left( c + (\langle \sigma(\vec{y}) \rangle - c) \right) \\ &= c^2 + c \left( (\langle \sigma(\vec{x}) \rangle - c) + (\langle \sigma(\vec{y}) \rangle - c) \right). \end{aligned} \quad (12)$$

Performing now the sample average, we have

$$\begin{aligned} \langle F_{\vec{x}_1 \rightarrow \vec{x}_2} \rangle &= v_{\vec{x}_2-\vec{x}_1} \left( \langle \sigma(\vec{x}_2) - \sigma(\vec{x}_1) \rangle \left( 1 - \frac{\Delta E_S(\vec{x}_1, \vec{x}_2, \sigma)}{k_B T} \right) \right. \\ &\quad \left. + \langle \frac{\Delta U(\vec{x}_1, \vec{x}_2, \sigma)}{2k_B T} \rangle \langle \sigma(\vec{x}_1) + \sigma(\vec{x}_2) - 2\sigma(\vec{x}_1)\sigma(\vec{x}_2) \rangle \right) \\ &= v_{\vec{x}_2-\vec{x}_1} \left( \langle \sigma(\vec{x}_2) - \sigma(\vec{x}_1) \rangle + \frac{\langle \Delta U(\vec{x}_1, \vec{x}_2, \sigma) \rangle}{k_B T} c(1-c) \right). \end{aligned} \quad (13)$$

where the first equality was due to neglecting correlations, i.e. terms of  $O((E/k_B T)^2)$ , and the second due to neglecting terms of  $O(1/N)$ . Taking account of all possible exchange vectors  $\vec{s}$ , we have

$$\frac{d}{dt} \langle \sigma(\vec{x}) \rangle = \sum_{\vec{s}} v_{\vec{s}} \left( \langle \sigma(\vec{x} + \vec{s}) - \sigma(\vec{x}) \rangle + \frac{\langle \Delta U(\vec{x}, \vec{x} + \vec{s}, \sigma) \rangle}{k_B T} c(1-c) \right). \quad (14)$$

We would now want to use this expression to describe the temporal evolution of a given state  $\sigma$  over time. The key to be able to do that is the observation that averaging the occupations of a given site  $\vec{x}$  over  $N$  systems (as we have assumed) is equivalent to averaging the occupations of  $N$  sites in one system. This can be exploited by changing over into reciprocal space, as the Fourier transform sums over all sites in the system. We therefore get

$$\frac{d}{dt} \langle A(\vec{q}) \rangle = \langle A(\vec{q}) \rangle \sum_{\vec{s}} v_{\vec{s}} (\cos(\vec{q}\vec{s}) - 1) \left( 1 + \frac{2\hat{V}(\vec{q})c(1-c)}{k_B T} \right), \quad (15)$$

with  $\hat{V}$  the Fourier transform of the pair potential  $V$ . The imaginary part cancels due to the inversion symmetry of the Bravais lattice. Comparing this result with (4) allows us to identify the coherent linewidth

$$\Gamma_{\text{coh}}(\vec{q}) = \sum_{\vec{s}} v_{\vec{s}} (1 - \cos(\vec{q}\vec{s})) \left( 1 + \frac{2\hat{V}(\vec{q})c(1-c)}{k_B T} \right). \quad (16)$$

We further observe that with the result of [Chudley and Elliott \(1961\)](#) for the incoherent linewidth

$$\Gamma_{\text{inc}}(\vec{q}) = \sum_{\vec{s}} v_{\vec{s}} (1 - \cos(\vec{q}\vec{s})) \quad (17)$$

and the connection between weak short-range interactions and the scattered intensity due to [Clapp and Moss \(1966\)](#) (see also the appendix for a quick derivation of this result)

$$I_{\text{SRO}}(\vec{q}) = \left( 1 + \frac{2\hat{V}(\vec{q})c(1-c)}{k_B T} \right)^{-1} \quad (18)$$

we arrive at the remarkably simple result

$$\Gamma_{\text{coh}}(\vec{q}) = \frac{\Gamma_{\text{inc}}(\vec{q})}{I_{\text{SRO}}(\vec{q})}. \quad (19)$$

In particular the coherent linewidth is equal to the incoherent linewidth for vanishing interactions, which was to be expected, as incoherent scattering is actually nothing else than coherent scattering from the (non-interacting) different isotopes/spin states.

The fact that the relaxation of fluctuations (i.e. the decay of the coherent intermediate scattering function) becomes slower

than the Chudley-Elliott value for positions in reciprocal space with high intensity (or equivalently the quasi-elastic line becomes narrower) has been known qualitatively under the name de Gennes-narrowing (de Gennes, 1959) from studies of liquids and colloidal glasses (Dasannacharya and Rao, 1965; Caronna et al., 2008). It is not difficult to understand: a high  $I_{\text{SRO}}(\vec{q})$  means that the particles prefer to build local arrangements corresponding to a high Fourier component at  $\vec{q}$ . The reason can only be that such arrangements are energetically favoured compared to other arrangements, therefore it takes more energy to break such arrangements up, making them longer-lived. However, the fact that in first order only the static interactions modify the linewidth (as opposed to deviations from the mean saddle-point energy) is not so obvious. From the experimentalist's point of view this means that the information accessed in a coherent experiment where the dynamics correspond to this high-temperature theory is equivalent to the information from an incoherent one. The simulations in the next section elucidate what happens when the approximations invoked here break down.

#### 4. The regime of stronger interactions as probed by simulations

Here we explore the range of validity of the theory developed in the previous section via computer simulations. We use a generic model of a binary system on the face-centred cubic lattice with a tendency to  $L1_2$ -ordering. This is inspired by the case of  $\text{Cu}_{90}\text{Au}_{10}$  (Schönfeld et al., 1999), which will also be the subject in section 5, but we think that the conclusions drawn here have general validity.

We performed Monte Carlo-simulations in the canonical ensemble. From the static point of view, the system is specified by the Hamiltonian (3). In order to capture the essence of the problem, we took only the first two interaction parameters as given by Schönfeld et al. (1999) for the potential  $V$ , i.e. a repulsive energy of  $J$  for nearest neighbours, and an attractive energy of  $0.256J$  for next-nearest neighbours. The concentration was fixed to  $c = 0.1$ , the size of the simulation cell was  $32 \times 32 \times 32$  face-centred cubic cells, i.e.  $N = 131072$  lattice sites. We used temperatures of  $k_{\text{B}}T = 2J$  and  $k_{\text{B}}T = J$ . With the interaction parameters of  $\text{Cu}_{90}\text{Au}_{10}$ , these values correspond to actual temperatures of 1061 K and 530 K, respectively.

We implemented the Monte Carlo-update, i.e. the transition from one microstate to the next, via exchanging the occupancy of neighbouring sites, which is known under the term Kawasaki dynamics in the solid-state Monte Carlo community. This is in contrast to diffusion in actual systems, where diffusion is in general mediated by the random walk of vacancies, leading to correlations in the jumps of the atoms, which results in an apparent distribution of the length of the atomic jumps (Wolf, 1977). This was the main reason for neglecting vacancies in our simulations, as it would unnecessarily complicate the picture. However, there is a physical scenario where our implementation would be correct from the ‘‘coherent’’ viewpoint: If the minority atoms have a much smaller jump frequency than the majority atoms, the vacancy will

cover large distances on the percolating majority sites between minority jumps, leading to vanishing correlations.

Equation (16) suggests  $1/\sum_{\vec{s}} v_{\vec{s}}$  as the natural timescale of the dynamics. In the high-temperature limit this corresponds to the time within which  $Nc(1-c)$  exchanges of occupancy of neighbouring atoms are executed, which we adopt in the following as the time unit.

The only ingredient left to specify is the choice of  $\Delta E_{\text{S}}$ , the saddle point energy deviations as a function of the surroundings as defined in section 3. We use three different models:

- $\Delta E_{\text{S}}(\vec{x}_1, \vec{x}_2, \sigma) = 0$ : We will call the model corresponding to this choice the midpoint model, as the saddle point energy is the average of initial and final energy plus a constant. Jumps leading to higher energies become progressively less probable, jumps to lower energies more probable.
- $\Delta E_{\text{S}}(\vec{x}_1, \vec{x}_2, \sigma) = |\Delta U(\vec{x}_1, \vec{x}_2, \sigma)|/2$ : In this model the saddle point energy is a constant plus the larger value among initial and final energy. The jump frequencies to higher energies are proportional to the Boltzmann factor of the energy difference, whereas downhill jumps have all the same frequency. This model is therefore equivalent to the well-known Metropolis algorithm (Metropolis et al., 1953).
- $\Delta E_{\text{S}}(\vec{x}_1, \vec{x}_2, \sigma) = -|\Delta U(\vec{x}_1, \vec{x}_2, \sigma)|/2$ : This is just the inverse of the Metropolis model, here all uphill jumps have the same (low) probability, whereas the downhill jumps have increasing probability with increasing energy difference. We will call this model the inverse Metropolis model.

All these models depend only on the difference in energy between initial and final state, whereas in actual solid state systems the saddle point energy is most likely significantly influenced by the occupancies of the sites making up the window the jumping atom has to pass through (Leitner et al., 2010). Our choices are nonetheless well suited to our aim of deriving basic insights into atomic-scale diffusion from the ‘‘coherent’’ viewpoint, as they do not depend on additional parameters describing interaction energies.

It is no coincidence that most Monte Carlo studies of static properties use the Metropolis algorithm, as it is the most efficient choice in the sense that the proportion of rejected jumps is lowest. With the midpoint or the inverse Metropolis model, even jumps between states of equal energy are necessarily rejected with a certain probability, as there has to be a margin for the increased acceptance probability of downhill jumps. Nevertheless, there is an energy threshold where the acceptance probability of downhill jumps reaches unity. In order to satisfy the principle of detailed balance, we accordingly decreased the acceptance probability of the corresponding uphill jumps. Choosing the acceptance probability of equal energy-jumps low enough, we managed to keep the proportion of jumps with energy differences below the threshold as low as 1% even in the case of the inverse Metropolis model at the lower temperature. This does not impact runtime much as the computation of the discrete Fourier transform uses more CPU time anyway.

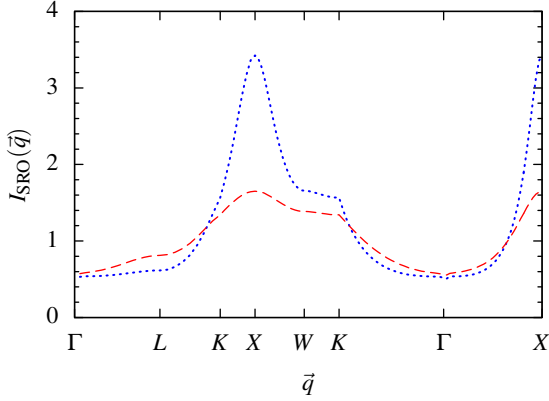


**Figure 1:** Short-range order scattering in Laue units for  $k_B T = 2J$  (dashed red) and  $k_B T = J$  (dotted blue).

In the visualization of the results of our simulations, the short-range order intensity  $I_{\text{SRO}}(\vec{q})$  and coherent linewidth  $\Gamma_{\text{coh}}(\vec{q})$ , we concentrate on the edges of the irreducible part of the first Brillouin zone of the face-centred cubic lattice. This is because we expect the observable features to be most pronounced at these extreme positions in reciprocal space.

The simulated short-range order intensities for both temperatures are given in figure 1. The values for the different models for the transition frequencies agree perfectly (which is a necessary criterion for the correctness of our implementation), we therefore plot the average of all the three models. The observed behaviour is consistent with the picture of a short-range ordered system with a tendency for  $L1_2$ -ordering: At lower temperatures the intensity peaks at the  $X$ -point, which is where the super-structure reflection of the  $L1_2$ -order would appear.

The analysis of the dynamics is performed by computing the Fourier transform of the scatterer density at regular time intervals and taking the average of the product of the amplitude at time  $t$  and the complex conjugate of the amplitude at time  $t + \Delta t$ . This directly gives the intermediate scattering function  $I(\vec{q}, \Delta t)$ , which is also known as the amplitude auto-correlation function in the photon correlation spectroscopists' community. The time dependence of the intermediate scattering function

should be an exponential decay due to (6). In our simulations this is not strictly the case, rather it generally appears as a so-called stretched exponential decay, i.e. as if corresponding to a distribution of decay times. For the following evaluation, we nevertheless fitted it by an exponential with one defined correlation time. We will discuss the deviations below.

The simulated coherent linewidths (or inverse of the correlation times) are given in figure 2. Just as with the short-range order intensity, at lower temperatures the features in the coherent linewidth as a function of wavevector transfer become more pronounced, and the qualitative finding of smaller linewidths where the intensity is high is clearly visible. The first point to note is that for higher temperatures the observed dynamics tends to be the same irrespective of the model for the saddle point energies as was predicted in section 3. At lower temperatures, however, the differences between the models become appreciable. This is not surprising, as the theory developed in section 3 is strictly valid only in the limit of weak interactions. Using the modulations in the observed short-range order scattering as a measure of the strength of the interactions, the case of  $k_B T = J$  is clearly outside the regime of weak interactions.

Computing the actual theoretical expression for the coherent linewidth due to (19) by using the simulated short-range order intensity yields the solid black lines in figure 2. Note however that we have scaled the theoretical value by a factor of 0.91 in the case of  $k_B T = 2J$  and by a factor of 0.71 in the case of  $k_B T = J$ . With these values the theoretical curves coincide nearly perfectly with the curves pertaining to the inverse Metropolis model. The other models give relaxations which are generally faster than with the inverse Metropolis model, and it can also be seen that it is not possible to bring the theoretical curve to agree with one of the other models by scaling with a constant factor alone, as the features there are more pronounced.

We will now discuss these observations. The interpretation of the results in section 3 was that energetically favourable local configurations are harder to break up (leading to longer lifetimes) and more numerous (leading to high short-range order scattering). The breaking-up has to happen via nearest-neighbour jumps of the atoms. When the degree of short-range order is high, we can expect the neighbouring states to be

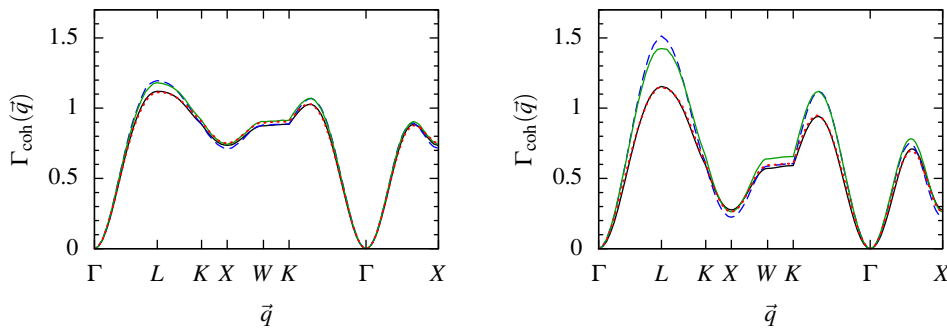


**Figure 2:** Coherent linewidth for  $k_B T = 2J$  (left panel) and  $k_B T = J$  (right panel) under the various transition models: Metropolis model (dashed blue), midpoint model (solid green), and inverse Metropolis model (dotted red), together with the theoretical expression due to (19) (solid black).

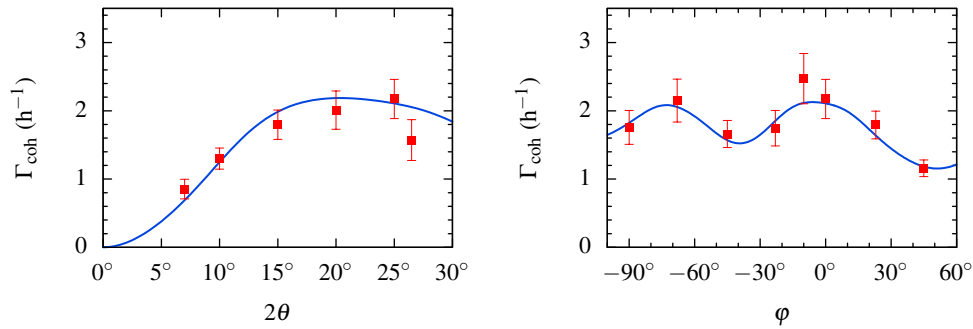


**Figure 3:** Fitted experimental linewidths at 543 K together with theoretical value. Scan over the scattering angle for fixed azimuthal angle at  $\varphi = 0^\circ$  (left panel), scan over the azimuthal angle for fixed scattering angle  $2\theta = 25^\circ$  (right panel).

energetically unfavourable. Contrary to what our mean-field theory of section 3 assumes, the energy necessary for breaking up a configuration is therefore not only the energy stored in the configuration relative to an average configuration, but also what is needed for traversing the barrier states. This explains why the theory underestimates the modulations in the coherent linewidth. We can now also understand why it fits best with the inverse Metropolis model: there the transition frequency between two states does not depend on the energy of the higher state, therefore the system can easily jump out of a low-energy state into a high barrier state, and if the second jump lowers the energy again, the system has a high probability of leaving the initial low-energy state permanently. If there is no alternative way down after the first jump, however, it will just reverse back into the initial state. This is now also the explanation why the relaxations in the inverse Metropolis model are slower than in the other models with the same number of exchanges and slower by a factor of 0.71 than in the theory: in this model quite a number of jumps are to states of very high energy that are reversed at the next opportunity.

The qualitative behaviour of the deviations of the decays of the simulated intermediate scattering function from true exponential decays supports this interpretation: The general trend is that they are less severe for higher temperatures, which is where the linear theory is increasingly valid, they are least for the inverse Metropolis model and highest for the Metropolis model due to above reasoning, and they are highest at the  $X$ -point with its high short-range order intensity and least for small  $\vec{q}$  around the  $\Gamma$ -point, which are not affected by short-range correlations.

## 5. Application to the interpretation of a recent XPCS experiment

Contrary to quasi-elastic neutron scattering, which has been used for determining atomic-scale dynamics since the 1960s (Sköld and Nelin, 1967), the insufficient available intensity of coherent x-rays has prohibited the application of x-ray photon correlation spectroscopy (XPCS) to this problem for a long time. It has been accomplished for the first time only recently in an experimental study of  $\text{Cu}_{90}\text{Au}_{10}$ , a system with strong diffuse scattering. Here we interpret the findings of this

experiment in the light of the results of the previous sections.

The system of Cu-Au exhibits the intermetallic phase  $\text{Cu}_3\text{Au}$ , which is probably the best known example of an  $L1_2$ -phase. In this phase the nearest neighbours of a Au atom are exclusively Cu, while the second-nearest neighbours are exclusively Au. A Au concentration of 10% is too small to maintain this long-range ordered phase at experimentally accessible temperatures, but the resulting alloy displays short-range order analogous to the  $L1_2$ -phase: the concentration of Au atoms on the nearest neighbour sites of a Au atom is much smaller than the overall Au concentration, whereas it is higher on the second-nearest neighbours (Schönfeld et al., 1999).

The experiment was performed at beamline ID10A at the ESRF in Grenoble, France. For experimental details we refer the reader to the principal publication (Leitner et al., 2009). The measurements were done with an incident photon energy of 8 keV, the single crystalline sample foil was mounted in transmission geometry at temperatures around 540 K. The scattered radiation was detected by a CCD-camera. The sample was kept fixed during the experiment, varying the wavevector transfer  $\vec{q}$  was achieved by changing the position of the camera via the scattering angle  $2\theta$  and the azimuthal angle  $\varphi$ . Data analysis was done by computing the auto-correlation function and subsequent fitting with a single exponential decay.

The fitted linewidths (inverse of the decay time) are given in figure 3. The theoretical curve was computed by the linear theory of (19) with the short-range order intensity as parameterized by Schönfeld et al. (1999) for this crystal and temperature range. The sample orientation was such that the  $(1\bar{1}0)$ -plane was perpendicular to the incident radiation, with the  $[001]$ -direction at an azimuthal angle of  $\varphi = 51^\circ$ . With a modulus of  $\vec{q}$  of  $1.75 \text{ \AA}^{-1}$  at a scattering angle of  $2\theta = 25^\circ$ , the path in the right panel of figure 3 is roughly on the boundary of the first Brillouin zone, and it passes near the  $X$ -point at  $\varphi = 51^\circ$ , the  $L$ -point at  $\varphi = -4^\circ$ , and the  $K$ -point at  $\varphi = -39^\circ$ . These special points correspond to the extrema of the linewidth and are in agreement with figure 2.

The experimental results and the theoretical curve in figure 3 show no significant disagreement. In the light of section 4 this is surprising, as the temperature in the experiment is very near the lower temperature of the simulations (530 K). Two points that explain the absence of deviations from the theory

in the experiment as opposed to the simulations can be put forward: first, the path passes only near the special points and not exactly through them, which is where we expect the deviations to be most pronounced, and second, we used in our simulations only the first two interaction parameters while it seems that the further parameters act as antagonists to the first two, as the maximum of the diffuse intensity as reported by Schönfeld et al. (1999) is only 2.4 Laue units, as opposed to our value of 3.5 Laue units. Given these two points, we do not claim that the dynamics in the sample is definitely described by the inverse Metropolis model, but we think it justifiable to assume that the actual dynamics is not wildly different from the midpoint model or the inverse Metropolis model.

## 6. Conclusion

In this paper we have given a simple derivation of the effect of interactions between the atoms on the coherent linewidths/correlation times in the high-temperature limit. These experimental quantities are accessible by coherent quasi-elastic neutron scattering or x-ray photon correlation spectroscopy. The application of the latter method to the measurement of atomic-scale diffusive dynamics in alloys is only very recent, but due to the rapid improvement of available coherent x-ray sources it has a great potential.

The main contribution of this work is to complement the high-temperature theory by Monte Carlo-simulations of a short-range ordered system at lower temperatures or equivalently stronger interactions, which is of relevance for the application to the interpretation of actual experiments. Specifically we found that for lower temperatures the signal becomes sensitive to the actual transition frequencies between states of the system. We have demonstrated this point by using rather academic models that depend only on the energy difference of initial and final state, but we are confident that this holds also for more physical models, where the transition frequency depends on the configuration of the window the jumping atom has to pass through. To our knowledge, such information has not yet been experimentally determined.

We have interpreted the findings of the first successful XPCS experiment on atomic diffusion. We found that the obtained correlation times correspond surprisingly well to the theory, even though the strength of the interactions is in a range where deviations should become visible. This is an indication that the actual transition frequencies do not differ too much from the ones in our models.

With the availability of improved x-ray sources it will become possible to conduct such experiments with a much improved statistical accuracy, which would then allow to draw definitive conclusions on the microscopic mechanisms in alloys beyond simple jump vectors and frequencies.

## Acknowledgments

We want to thank Lorenz-Mathias Stadler and Bastian Pfau, our coworkers with the experiment, and especially Bogdan Sepiol, whose participation was essential to the success of this

work. Michael Leitner acknowledges support by the Austrian Science Fund (FWF): P22402.

## Appendix

Here we give a proof of the so-called Clapp-Moss-relation (18), which is a simple expression linking the pair potential and the observable short-range order intensity. For the range of validity needed here it is just a corollary of the results derived in section 3. The main concept here is to describe a state by its scattering amplitude for a given  $\vec{q}$ , which is a random variable in the complex plane, and to compute the stochastic equations describing the time evolution of this variable.

Take a state  $\sigma$  from the canonical ensemble. The crystal is assumed to be short-range ordered, with a correlation length on the order of unity. Regions in the crystal which are farther apart can therefore be considered as independent. As a consequence, the distribution of the scattering phases of the single particles on the unit circle is approximately uniform, the deviations vanish as the crystal size goes to infinity.

We now let one particle jump by a vector  $\vec{s}$  and compute the variance of the real part of the scattering amplitude of the system after the jump, i.e. the variance of the difference of the contributions of the jumping particle:

$$v_s^r = \left\langle \left( \cos(\vec{q}(\vec{x} + \vec{s})) - \cos(\vec{q}\vec{x}) \right)^2 \right\rangle = 1 - \cos(\vec{q}\vec{s}) \quad (\text{A.1})$$

The jump probabilities are denoted by  $v_s$  in the nomenclature of section 3, we therefore obtain for the increase in variance of the probability distribution of the system's scattering amplitude over time

$$\frac{d}{dt} V(A^r(\vec{q})) = C \sum_{\vec{s}} v_s v_s^r = C \Gamma_{\text{inc}}(\vec{q}), \quad (\text{A.2})$$

the same holds for the imaginary part. The constant  $C$  will be specified later on. This result holds only for small times as the second jump of a particle would be strongly correlated with the first.

Together with the regression of the expected value of the distribution (15) the above equation specifies the temporal evolution of the probability distribution of the scattering amplitude. In the long-time limit it will evolve to a Gaussian distribution centred at the origin. The variance in the real coordinate  $V^r$  of this equilibrium distribution can be computed by requiring stationarity:

$$0 = \frac{d}{dt} V^r = C \Gamma_{\text{inc}}(\vec{q}) - 2V^r \Gamma_{\text{coh}}(\vec{q}), \quad (\text{A.3})$$

equally for  $V^i$ . The expected value of the intensity is the sum of the variances in both dimensions, therefore

$$I_{\text{SRO}}(\vec{q}) = C \frac{\Gamma_{\text{inc}}(\vec{q})}{\Gamma_{\text{coh}}(\vec{q})} = \frac{C}{1 + \frac{2\hat{V}(\vec{q})c(1-c)}{k_B T}}. \quad (\text{A.4})$$

To compute the normalization constant  $C$ , we observe that in Laue units the diffuse intensity of a random occupation without short-range order is equal to unity. Due to the unitarity

of the Fourier transform the summed diffuse intensity over the Brillouin zone is equal to the number of particles, in particular it is independent of the configuration as long as the concentration is fixed. Therefore  $C$  has to be chosen such that the integral over the whole Brillouin zone has the correct value. This is just the result of [Clapp and Moss \(1966\)](#).

Considering the high-temperature limit, the integral over  $\widehat{V}(\vec{q})$  is zero as a particle does not interact with itself. For vanishing interactions we have  $C = 1$ , therefore  $C = 1 + O((E/k_B T)^2)$ .

## References

- Caronna C, Chushkin Y, Madsen A and Cupane A 2008 *Phys. Rev. Lett.* **100**, 055702.
- Chudley C T and Elliott R J 1961 *Proc. Phys. Soc. London* **77**, 353–361.
- Clapp P C and Moss S C 1966 *Phys. Rev.* **142**, 418–427.
- Cook J C, Richter D, Scharpf O, Benham M J, Ross D K, Hempelmann R, Anderson I S and Sinha S K 1990 *J. Phys.: Condens. Matter* **2**, 79–94.
- Dasannacharya B A and Rao K R 1965 *Phys. Rev.* **137**, A417–A427.
- de Gennes P G 1959 *Physica* **25**, 825–839.
- Leitner M, Sepiol B, Stadler L M, Pfau B and Vogl G 2009 *Nature Mat.* **8**, 717–720.
- Leitner M, Vogtenhuber D, Pfeiler W and Püschl W 2010 *Intermetallics* **18**, 1091–1098.
- Metropolis N, Rosenbluth A W, Rosenbluth M N, Teller A H and Teller E 1953 *J. Chem. Phys.* **21**, 1087–1092.
- Petry W and Vogl G 1987 in ‘Materials Science Forum’ Vol. 15–18 Zürich: Trans Tech Publications pp. 323–348.
- Schönfeld B, Portmann M J, Yu S Y and Kosterz G 1999 *Acta Mater.* **47**, 1413–1416.
- Sinha S K and Ross D K 1988 *Physica B* **149**, 51–56.
- Sköld K and Nelin G 1967 *J. Phys. Chem. Solids* **28**, 2369–2380.
- Springer T and Lechner R E 2005 in P Heitjans and J Kärger, eds, ‘Diffusion in Condensed Matter’ Springer Berlin Heidelberg pp. 93–164.
- van Hove L 1954 *Phys. Rev.* **95**, 249–262.
- Vineyard G H 1957 *J. Phys. Chem. Solids* **3**, 121–127.
- Vogl G and Sepiol B 2005 in P Heitjans and J Kärger, eds, ‘Diffusion in Condensed Matter’ Springer Berlin Heidelberg pp. 65–91.
- Wolf D 1977 *Appl. Phys. Lett.* **30**, 617–619.